



Negative refraction without absorption via both coherent and incoherent fields in a four-level left-handed atomic system

Shun-Cai Zhao^{a,b,c}, Zheng-Dong Liu^{a,b,c,*}, Qi-Xuan Wu^d

^a School of Materials Science and Engineering, Nanchang University, Nanchang 330031, PR China

^b Engineering Research Center for Nanotechnology, Nanchang University, Nanchang 330047, PR China

^c Institute of Modern Physics, Nanchang University, Nanchang 330031, PR China

^d College English Department, Hainan University, Danzhou 571737, PR China

ARTICLE INFO

Article history:

Received 15 January 2010

Received in revised form 9 March 2010

Accepted 20 April 2010

Keywords:

Negative refraction

Without absorption

Coherent field

Incoherent field

ABSTRACT

This paper attempts a probe into negative refraction without absorption by means of an incoherent pump field and a strong coherent field coupling the dense four-level atomic system. With the application of the incoherent pump field to manipulate the populations in atomic levels and the variable strong coherent field to create quantum coherence, the constraint condition of two equal transition frequencies responding to the probe field in the atomic system isn't required. And these lead to the propagation transparency and strong magnetic response of the probe field, left-handedness with vanishing absorption in the atomic system. However, an excessive coherent field intensity would increase the absorption.

© 2010 Elsevier B.V. All rights reserved.

1. Introduction

Negative refraction of electromagnetic radiation [1] has recently attracted considerable attention because of its surprising and counterintuitive electromagnetic and optical effects, such as the reversals of both Doppler shift and Cherenkov effect, negative refraction [2], amplification of evanescent waves [3] and subwavelength focusing [3–5], negative Goos–Hänchen shift [6] and quenching spontaneous emission [7,8] and so on [9]. And material with negative refraction index intrigues the researchers because of its many significant potential applications. The “perfect lens” is one of them. Since a slab of such materials has an ability to focus all frequency components of a two-dimensional image, it may become possible to make a “perfect lens” in which imaging resolution is not limited by the diffraction limit [3]. Up to now, there have been several approaches to the realization of negative refractive index materials, including artificial composite metamaterials [10,11], photonic crystal structures [12], transmission line simulation [13] and chiral media [14,15] as well as photonic resonant materials (coherent atomic vapour) [16–19]. In such a type of negative refractive materials, negative refraction is usually accompanied by a strong absorption especially towards higher frequencies. Thus, the realization of negative refraction material without absorption is of great significance. And some effort [20–23] has been made to realize negative refraction without absorption. Kästel et al. [20]

realized negative refraction with minimal absorption in a dense atomic gas via electromagnetically induced chirality. The key ingredient of the scheme is the electromagnetic chirality that results from coherently coupling a magnetic dipole transition with an electric dipole transition via atomic coherence induced by the two-photon resonant Raman transitions. In Ref. [21], Kästel et al. also discussed negative refraction with reduced absorption due to destructive quantum interference in coherently driven atomic media. The negative refraction with deeply depressing absorption and without simultaneously requiring both negative electric permittivity and magnetic permeability (left-handedness) [2] was obtained by F.L. Li [23]. Ref. [23] shows this at the ideal situation that the two chirality coefficients have the same amplitude but the opposite phase.

In this paper we propose an indirect coupling way of the atoms responding to the probe field via an incoherent pump field and a coherent coupling field. With the application of the incoherent pump field to manipulate the population distribution of each level and the variable coherent field to create quantum coherence, the magnetic response is amplified and the probe field propagates transparently. The atomic system displays a negative refraction without absorption and left-handedness. The constraint condition of two equal transition frequencies responding to the probe field is not required, which is different from Ref. [18,24].

2. Theoretical model

The level configuration of atoms under consideration is shown in Fig. 1. The properties of the four atomic states are as follows: levels $|1\rangle$, $|3\rangle$, and $|4\rangle$ have the same parity, and the parity of level $|2\rangle$ is opposite

* Corresponding author. School of Materials Science and Engineering, Nanchang University, Nanchang 330031, PR China.

E-mail addresses: zscnum1@126.com, lzdgroup@ncu.edu.cn (Z.-D. Liu).

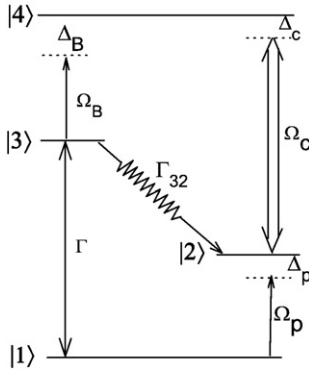


Fig. 1. Four-level atomic medium interacting with a coherent Ω_C , an incoherent pump Γ and a probe field Ω_P .

with theirs. The two lower levels $|1\rangle$ and $|2\rangle$ have opposite parity and so $\langle 2|\vec{d}|1\rangle \neq 0$ where \vec{d} is the electric dipole operator. The two upper levels, $|3\rangle$ and $|4\rangle$ have the same parity with $\langle 4|\vec{\mu}|3\rangle \neq 0$ where $\vec{\mu}$ is the magnetic dipole operator. As observed in Fig. 1, three electromagnetic fields are introduced to couple the four states: the electric and magnetic components of the probe light (corresponding Rabi frequency $\Omega_P = \frac{E_P d_{21}}{\hbar}$, $\Omega_B = \frac{B_P \mu_{43}}{\hbar}$) interact with the transitions $|2\rangle$ and $|1\rangle$ as well as $|4\rangle$ and $|3\rangle$, respectively. The incoherent pump field with pumping rate denoted by Γ pumps atoms in level $|1\rangle$ into the upper level $|3\rangle$, and then the atoms decay into metastable level $|2\rangle$ via rapid nonradiative transitions, whose decay rate is denoted as Γ_{32} . The strong coherent field Ω_C takes two effects on the system: (i) populations in level $|2\rangle$ are being pumped into level $|4\rangle$ and causes population reversion gain for magnetic dipole transition $|3\rangle \leftrightarrow |4\rangle$; (ii) quantum coherence is induced by it and causes energy levels $|2\rangle$ and $|4\rangle$ split into two dressed sublevels and results in enough response of the electric part of probe field at certain frequency extent.

Using the density matrix approach, the time-evolution of the system is described as

$$\frac{d\rho}{dt} = -\frac{i}{\hbar}[H, \rho] + \Lambda\rho, \quad (1)$$

Where $\Lambda\rho$ represents the irreversible decay part in the system. Under the dipole approximation and the rotating wave approximation the density matrix equations described the system are written as follows:

$$\dot{\rho}_{11} = \Gamma(\rho_{33} - \rho_{11}) + \Gamma_{21}\rho_{22} + \Gamma_{31}\rho_{33} + \Gamma_{41}\rho_{44} + i\Omega_P(\rho_{21} - \rho_{12}), \quad (2)$$

$$\dot{\rho}_{21} = -(\gamma_{21} + i\Delta_P)\rho_{21} - i\Omega_P(\rho_{22} - \rho_{11}) + i\Omega_C\rho_{41}, \quad (3)$$

$$\dot{\rho}_{22} = -\Gamma_{21}\rho_{22} + \Gamma_{32}\rho_{32} + \Gamma_{42}\rho_{44} + i\Omega_P(\rho_{12} - \rho_{21}) + i\Omega_C(\rho_{42} - \rho_{24}), \quad (4)$$

$$\dot{\rho}_{31} = -[\gamma_{31} + i(\Delta_C + \delta)]\rho_{31} + i\Omega_P\rho_{23} + i\Omega_B\rho_{41}, \quad (5)$$

$$\dot{\rho}_{32} = -[\gamma_{32} + i(\Delta_C - \Delta_P + \delta)]\rho_{32} - i\Omega_C\rho_{34} - i\Omega_P\rho_{31} + i\Omega_B\rho_{42}, \quad (6)$$

$$\dot{\rho}_{33} = -\Gamma(\rho_{33} - \rho_{11}) - \Gamma_{31}\rho_{33} - \Gamma_{32}\rho_{33} + \Gamma_{43}\rho_{44} + i\Omega_B(\rho_{43} - \rho_{34}), \quad (7)$$

$$\dot{\rho}_{41} = -[\gamma_{41} + i(\Delta_P + \Delta_C)]\rho_{41} + i\Omega_C\rho_{21} - i\Omega_P\rho_{42} + i\Omega_B\rho_{31}, \quad (8)$$

$$\dot{\rho}_{42} = -(\gamma_{42} + i\Delta_C)\rho_{42} + i\Omega_C(\rho_{22} - \rho_{44}) - i\Omega_P\rho_{41} + i\Omega_B\rho_{32}, \quad (9)$$

$$\dot{\rho}_{43} = -[\gamma_{43} + i(\Delta_P - \delta)]\rho_{43} + i\Omega_C\rho_{23} + i\Omega_B(\rho_{33} - \rho_{44}), \quad (10)$$

where the above density matrix elements obey the conditions: $\rho_{11} + \rho_{22} + \rho_{33} + \rho_{44} = 1$ and $\rho_{ij} = \rho_{ji}^*$. And Γ_{ij} ($i, j = 1, 2, 3, 4$) is the spontaneous emission decay rate from level $|i\rangle$ to level $|j\rangle$, ignoring the collision

broaden effect. $\gamma_{21} = \Gamma_{21}/2$, $\gamma_{31} = (\Gamma_{31} + \Gamma_{32})/2$, $\gamma_{41} = (\Gamma_{43} + \Gamma_{42})/2$, $\gamma_{42} = (\Gamma_{43} + \Gamma_{31} + \Gamma_{21})/2$, $\gamma_{43} = (\Gamma_{43} + \Gamma_{42} + \Gamma_{31} + \Gamma_{32})/2$, $\gamma_{32} = (\Gamma_{32} + \Gamma_{31} + \Gamma_{21})/2$ are the decay rates to the corresponding transitions. The detuning of the fields defined as $\Delta_P = \omega_{21} - \omega_P$, $\Delta_C = \omega_{42} - \omega_C$, $\Delta_B = \omega_{43} - \omega_P$, respectively. $\omega_{ij} = \omega_i - \omega_j$ is the transition frequency of levels $|i\rangle$ and $|j\rangle$ ($i, j = 1, 2, 3, 4$) and we have $\delta = \Delta_P - \Delta_B$.

According to the classical electromagnetic theory, the electric polarizability is a rank 2 tensor defined by its Fourier transform $\vec{P}_e(\omega_P) = \epsilon_0 \alpha_e(\omega_P) \vec{E}(\omega_P)$, which is calculated as the mean value of the atomic electric dipole moment operators by the definition $\vec{P}_e = \text{Tr}\{\rho \vec{d}\} = \rho_{12} d_{21} + \text{c.c.}$ where Tr stands for trace. In the following, we only consider the polarizability at the frequency ω_P of the incoming field \vec{E}_e . Therefore we drop the explicit ω_P dependence $\alpha_e(\omega_P) \equiv \alpha_e$. Moreover, we choose \vec{E}_e parallel to the atomic dipole \vec{d}_{21} so that α_e is a scalar, and its expression is as follows:

$$\alpha_e = \frac{\vec{d}_{21} \rho_{12}}{\epsilon_0 \vec{E}_P} = \frac{|d_{21}|^2 \rho_{12}}{\epsilon_0 \hbar \Omega_P}, \quad (11)$$

In the same way, the classical magnetic polarizations of the medium $\vec{P}_m(\omega_P) = \mu_0 \alpha_m \vec{E}_e(\omega_P)$, which is related to the mean value of the atomic dipole moment operator through $\vec{P}_m = \text{Tr}\{\rho \vec{\mu}\} = \rho_{34} \mu_{43} + \text{c.c.}$ According to the classical Maxwell's electromagnetic wavevector relation, we choose the magnetic dipole that is perpendicular to the induced electric dipole so that the magnetizability α_m is scalar, and its expression is as follows:

$$\alpha_m = \frac{\mu_0 \vec{\mu}_{43} \rho_{34}}{\vec{B}_P} = \frac{\mu_0 |\mu_{43}|^2 \rho_{34}}{\hbar \Omega_B}. \quad (12)$$

According to the Clausius–Mossotti relations considering the local effect in dense medium [25], the relative permittivity and relative permeability are expressed as [18,26]

$$\epsilon_r = \frac{1 + \frac{2}{3} N \alpha_e}{1 - \frac{1}{3} N \alpha_e}, \quad (13)$$

$$\mu_r = \frac{1 + \frac{2}{3} N \gamma_m}{1 - \frac{1}{3} N \gamma_m}. \quad (14)$$

In the above, we obtained the expressions for the electric permittivity and magnetic permeability of the atomic media. In the section that follows, we will demonstrate that both simultaneously negative permittivity and permeability, and negative refraction without absorption can be observed in the four-level atomic system.

3. Results and discussion

In the following, with the stationary solutions to the density matrix Eqs. (2)–(10), we explore the property of both simultaneously negative electric permittivity and magnetic permeability through the numerical calculations. And several typical parameters should be selected before the calculation. The parameters for the electric and magnetic polarizabilities of atoms can be chosen as: electric and magnetic transition dipole moments $d_{21} = 2.5 \times 10^{-29} \text{ C m}$ and $\mu_{34} = 7.0 \times 10^{-23} \text{ C m}^2 \text{ s}^{-1}$ [16], respectively. The density of atom N was chosen to be $6.5 \times 10^{25} \text{ m}^{-3}$ [27,28]. And the other parameters are scaled by $\gamma = 10^6 \text{ s}^{-1}$: $\Gamma_{31} = \Gamma_{41} = \Gamma_{42} = \Gamma_{43} = 0.01\gamma$, $\Gamma_{21} = 0.5\gamma$, $\Gamma_{32} = 1\gamma$. The Rabi frequency of the probe field is $\Omega_P = 0.5\gamma$, and $\delta = -20\gamma$ without the condition of the two transition frequencies $\omega_{43} = \omega_{21}$. The incoherent pumping rate is $\Gamma = 1.0\gamma$. The strong coherent optical field couples the atomic system with variational Rabi frequencies $\Omega_C = 15\gamma, 18\gamma, 21\gamma$, and 24γ and fixed frequency detuning $\Delta_C = 20\gamma$.

Fig. 2 shows the calculated electric permittivity ϵ_r and magnetic permeability μ_r as a function of probe field detuning. Under the

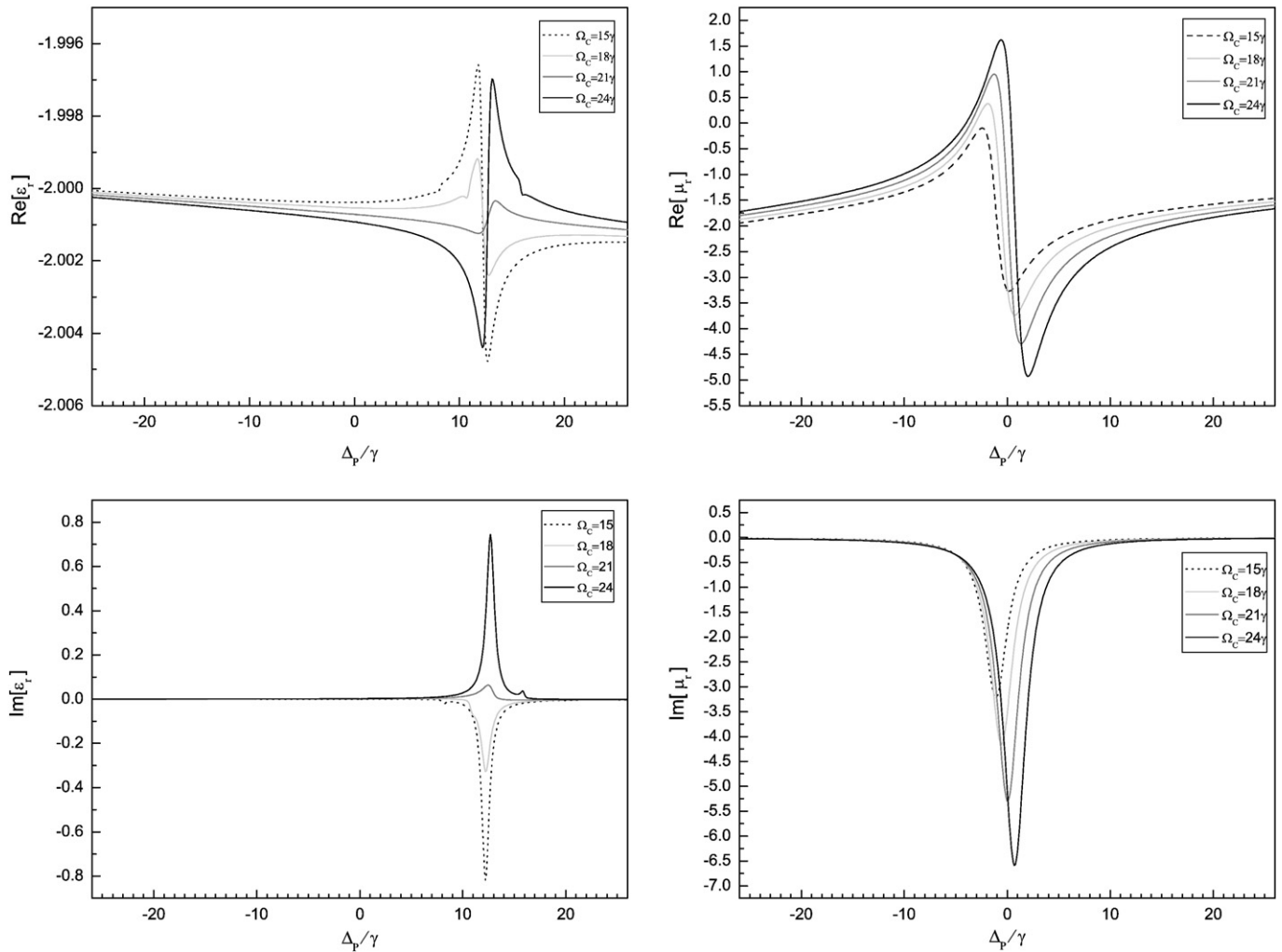


Fig. 2. The relative electric permittivity ϵ_r and magnetic permeability μ_r of the system as a function of probe frequency detuning Δ_p/γ for different values of Ω_c .

cooperation of the strong coherent field and incoherent pumping, the dense four-level atomic system exhibits left-handedness with simultaneously negative permittivity and permeability at some frequency extents of the probe field. From the profiles of the real part of the relative electric permittivity ϵ_r , we observe their values being proximately equal -2 in the probe frequency range $[-26\gamma, 26\gamma]$, although the phase of the figures are proximately opposite at $\Delta_p = 12.5\gamma$ when the Rabi frequency Ω_c varies by 15γ , 18γ , 21γ and 24γ . The influence of the strong coherent field on the real part of the relative magnetic permeability μ_r is different. When $\Omega_c = 15\gamma$, the value is all negative in the probe frequency extent. When $\Omega_c = 18\gamma$, 21γ , 24γ , the positive values emerge in the ranges of $[-3\gamma, -1.1\gamma]$, $[-3.4\gamma, -0.4\gamma]$, $[-3.85\gamma, 0.36\gamma]$, respectively. And their amplitude values are increasing with the variation of Ω_c . However, the ranges for simultaneously negative electric permittivity ϵ_r and magnetic permeability μ_r still exist. In Fig. 2, the transparency is shown by the imaginary part of both the relative electric permittivity ϵ_r and the relative magnetic permeability μ_r in some frequency extents. This is a very significant result for us. As is well known, the photon absorption of atom can be greatly depressed via electromagnetically induced transparency (EIT) [29]. And the zero absorption phenomena may occur in the EIT extents. With observation of the profile of the imaginary part of ϵ_r , the excessive strong coherent field intensity causes the shrinking gain and increasing absorption at $\Delta_p = 12.5\gamma$. However, the imaginary part of μ_r displays increasing gain, and its amplitude is gradually amplified and gradually approaching to the resonant point when the coherent field is varied the Rabi frequencies by 15γ , 18γ , 21γ and 24γ . Comparing the

images of the relative electric permittivity ϵ_r with the relative magnetic permeability μ_r in Fig. 2, we notice that the magnetic response of the probe field is stronger than the electric response. The reason may come from that: the magnetic component of the probe field couples levels $|4\rangle$ and $|3\rangle$, and the strong coherent field drives levels $|2\rangle$ and $|4\rangle$. The effect of quantum coherence caused by the strong coherent field on the magnetic component is stronger than on the electric component which couples levels $|2\rangle$ and $|1\rangle$.

In Fig. 3, the refraction index according to the definition of the left-handed material ($n(\omega) = -\sqrt{\epsilon_r(\omega)\mu_r(\omega)}$) [2] is plotted for different values of parameter Ω_c . As observed in Fig. 3, the real part of the refractive index shows negative values and their amplitudes enlarge gradually with the increasing of Ω_c . The imaginary part of the refractive index displays absorption enhancing near the resonant point and absorption depression on the both sides, when the coherent field is varied the Rabi frequencies by 15γ , 18γ , 21γ and 24γ . The figure of merit (FOM) $|Re(n)/Im(n)|$ shows how much the absorption is suppressed. When the FOM is much larger than unity, it means that there is almost no absorption in this area. As shown in Fig. 4, the FOM is far less than unity in the area near the resonant point. This illustrates that the increasing absorption occurs in this area, which is consistent with the peaks of $Im[n]$ near the resonance in Fig. 3. And the FOM has the largest value at the identical re-scaled detuning parameter Δ_p/γ when $\Omega_c = 15\gamma$. It means that the absorption is depressed deeply when the coherent field varies its Rabi frequency to $\Omega_c = 15\gamma$, and the excessive coherent field intensity wouldn't help to

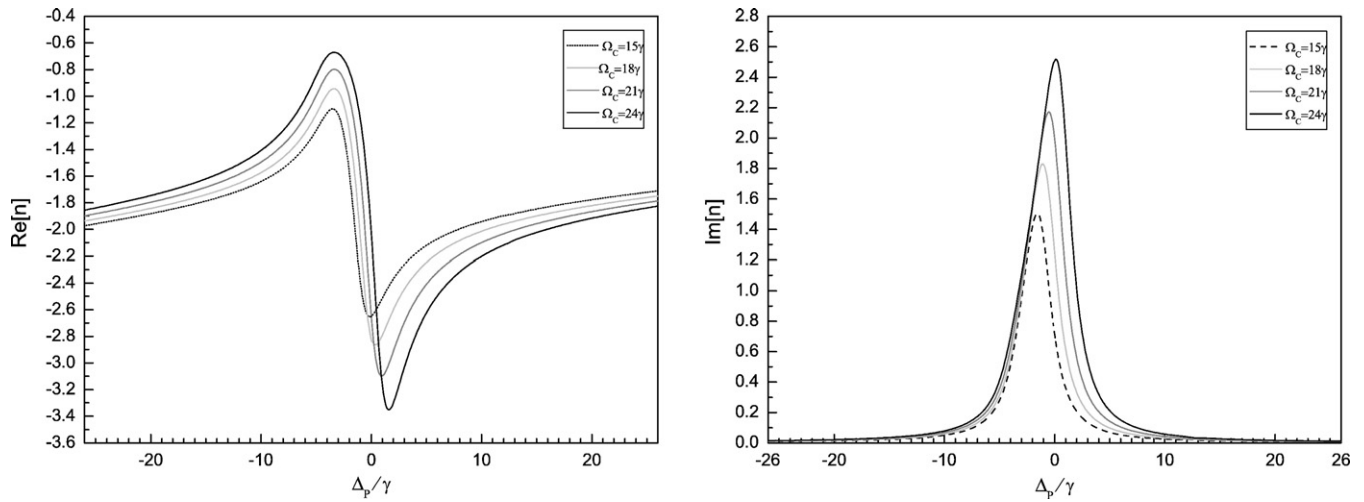


Fig. 3. The refractive index as a function of the probe field detuning Δ_p/γ for different values of Ω_c .

realize zero absorption. The markedly feature of present scheme is the absorption depression almost to zero in the left-handed atomic system. One may get the reason for this from the results shown in Fig. 2. Because of the EIT effect, the electric and magnetic non-absorption extents appear in the re-scaled detuning parameter Δ_p/γ extent, which brings about the zero value of the imaginary part of refraction index. As a result, the negative refraction without absorption occurs in the left-handed atomic system.

In experimental investigation, the solid sample of E_r^{3+} doped into calcium fluorophosphate at room temperature might be a good candidate because it has abundant energy levels, various electric magnetic transitions and high density in the order 10^{25} m^{-3} [27,28]. And the four levels $|1\rangle$, $|2\rangle$, $|3\rangle$, and $|4\rangle$ in Fig. 1 correspond to the energy level configuration $I_{15/2}^4$, $I_{13/2}^4$, $I_{9/2}^4$ and $I_{11/2}^4$ of the rare earth ion E_r^{3+} doped in calcium fluorophosphate, respectively.

4. Conclusion

In conclusion, we have demonstrated a scheme for realizing negative refraction without absorption via an incoherent pump field and a strong coherent field in the dense four-level atomic system. With the application of the incoherent pump field to manipulate the population distribution of each level and the variable strong coherent

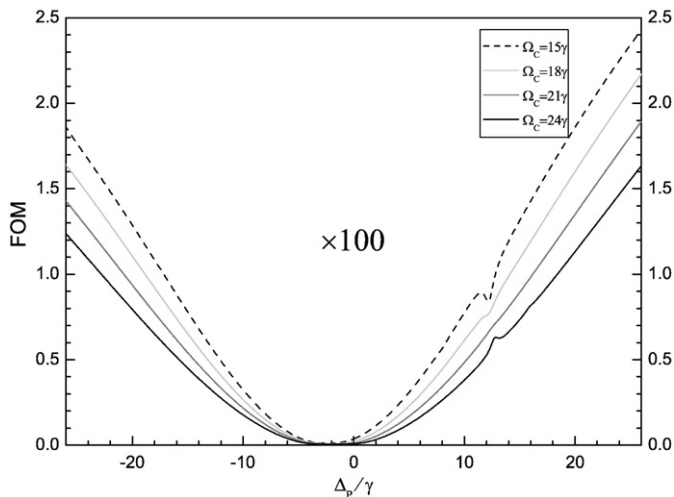


Fig. 4. The figure of merit (FOM: $|\text{real}(n)/\text{imag}(n)|$) as a function of the detuning parameter detuning Δ_p/γ for different values of Ω_c .

field to create quantum coherence, the magnetic response is amplified and the probe field propagates transparently in some frequency extents. Without the constraint condition of two equal transition frequencies responding to the probe field, the atomic system displays a negative refraction with vanishing absorption and left-handedness. Therefore, our aim for searching the low-loss negative refraction is possible by choosing appropriate parameters in the scheme, in respect that the main applied limitation of the negative refractive materials is the large amount of dissipation and absorption. However, an excess coherent field intensity would increase the absorption near the resonance. This can also be obviously observed here.

Acknowledgments

The work is supported by the National Natural Science Foundation of China (Grant No. 60768001 and No. 10464002).

References

- [1] M.O. Scully, M.S. Zubairy, Quantum Optics, Cambridge University Press, Cambridge, 1997.
- [2] V.G. Veselago, Sov. Phys. Usp. 10 (1968) 509.
- [3] J.B. Pendry, Phys. Rev. Lett. 85 (2000) 3966.
- [4] L. Chen, S. He, L. Shen, Phys. Rev. Lett. 92 (2004) 107404.
- [5] K. Aydin, I. Bulu, E. Ozbay, Appl. Phys. Lett. 90 (2007) 254102.
- [6] P.R. Berman, Phys. Rev. E 66 (2002) 067603.
- [7] Y.P. Yang, J.P. Xu, H. Chen, S.Y. Zhu, Phys. Rev. Lett. 100 (2008) 043601.
- [8] V. Yannopoulos, E. Paspalakis, N.V. Vitanov, Phys. Rev. Lett. 103 (2008) 063602.
- [9] Z.M. Zhang, C.J. Fu, Appl. Phys. Lett. 80 (2002) 1097.
- [10] R.A. Shelby, D.R. Smith, S. Schultz, Science 292 (2001) 77.
- [11] J. Pendry, Nature 423 (2003) 22.
- [12] E. Cubukcu, Nature 423 (2003) 604.
- [13] G.V. Eleftheriades, A.K. Iyer, P.C. Kremer, IEEE Trans. Microwave Theory Tech. 50 (2002) 2702.
- [14] J.B. Pendry, Science 306 (2004) 1353.
- [15] V. Yannopoulos, J. Phys. Condens. Matter 18 (2006) 6883.
- [16] Q. Thommen, P. Mandel, Phys. Rev. Lett. 96 (2006) 053601.
- [17] M.ö. Oktel, ö.E. Müteçaplı, Phys. Rev. A 70 (2004) 053806.
- [18] C.S. Zhao, D.Z. Liu, Int. J. Quant. Inf. 7 (2009) 747.
- [19] J.Q. Shen, Phys. Lett. A 357 (2006) 54.
- [20] J. Kästel, M. Fleischhauer, S.F. Yelin, R.L. Walsworth, Phys. Rev. Lett. 99 (2007) 073602.
- [21] J. Kästel, M. Fleischhauer, S.F. Yelin, R.L. Walsworth, Phys. Rev. A 79 (2009) 063818.
- [22] P. Tassin, L. Zhang, Th. Koschny, E.N. Economou, C.M. Soukoulis, Phys. Rev. Lett. 102 (2009) 053901.
- [23] F.L. Li, A.P. Fang, M. Wang, J. Phys. B 42 (2009) 199505.
- [24] H.J. Zhang, Y.P. Niu, S.Q. Gong, Phys. Lett. A 363 (2007) 497.
- [25] G.S. Agarwal, R.W. Boyd, Phys. Rev. A 60 (1999) R2681.
- [26] J.Q. Shen, J. Mod. Opt. 53 (2006) 2195.
- [27] A.A. Kaminskii, V. Mironov, S.A. Kornienko, S.N. Bagaev, G. Boulon, A. Brenier, B. Di Bartolo, Phys. Status Solidi A 151 (1995) 231.
- [28] D.K. Sardar, C.H. Coeckelenbergh, R.M. Yow, J.B. Gruber, T.H. Allik, J. Appl. Phys. 98 (2005) 033535.
- [29] N. Papasimakis, V.A. Fedotov, N.I. Zheludev, S.L. Prosvirnin, Phys. Rev. Lett. 101 (2008) 253903.